

CHAPTER IV
PREPARATION OF SILK FIBROIN/CELLULOSE WHISKERS
BIONANOCOMPOSITE SPONGES FOR YEAST CELL IMMOBILIZATION
USED IN CONTINUOUS ETHANOL PRODUCTION BY PACKED BED
BIOREACTOR

4.1 Abstract

Silk fibroin (SF)/cellulose whiskers (CLWs) bionanocomposite sponges were prepared as a supporting material for yeast cell immobilization for further using in continuous ethanol production. The SF/CLWs bionanocomposite sponges with high porosity were fabricated by freeze-drying a silk fibroin solution containing cellulose whiskers at different SF/CLWs weight ratios. The freeze-dried SF/CLWs sponges were subjected to methanol treatment to increase water stability. Increasing the CLWs content resulted in higher water stability, less shrinkage, and better mechanical properties of SF/CLWs bionanocomposite sponges. In the continuous ethanol fermentation process, the bionanocomposite sponges with a SF/CLWs weight ratio of 50/50 were used to immobilize *Saccharomyces cerevisiae burgundy* KY11 yeast cells. The bionanocomposite sponges with the immobilized yeast cells were loaded into the glass column of a packed bed bioreactor. Continuous ethanol fermentation was operated by varying D-glucose concentrations (100, 150, 200 g/l), dilution rates (0.15, 0.20, 0.25 hr⁻¹), and hydraulic retention times (6.87, 5.15, 4.12 hr). The continuous ethanol fermentation with a high concentration of D-glucose, low dilution rate, and high hydraulic retention time resulted in the production of a higher ethanol concentration.

Keywords: Silk fibroin; Cellulose whiskers; Yeast cell immobilization; Continuous ethanol fermentation

4.2 Introduction

In recent years, fuel oil demand is continually increased because of extended population in the world. On the other hand, natural source of fuel oil that is petroleum fuel is perpetually decreasing. Alcohol-based fuels are alternative energy sources which have been used as replacements for gasoline. Especially, ethanol fuel that is the most widely used due to its low toxicity and wide abundance is produced from renewable agricultural product, which is called “Bioethanol”. Ethanol can be directly used or blended with gasoline to any percentage such as 10% ethanol mixed with 90% gasoline is called E10. This blend is referred to “gasohol”. Blending ethanol with gasoline has several advantages: increasing octane value of gasoline, decreasing carbon monoxide emission and hydrocarbon exhaust.

Bioethanol means ethanol liquid biofuel which is produced from renewable agricultural sugar crops (sugar cane, molasses), corn, lignocellulosic (bagasse and wood) sources via hydrolysis and fermentation process. Fermentation process is more important to produce ethanol. Therefore, process of continuous ethanol fermentation in packed-bed bioreactor is considered in order to get high ethanol production. Moreover, cell immobilization is a technique that has been extensively investigated during few decades to enhance fermentation productivity.

Cell immobilization is more interesting. There are many advantages of cell immobilization over free cells such as high volumetric productivity of ethanol, relative ease of product separation, reusable of biocatalysts, important protection of biocatalysts from inhibitions (Bangrak, 2007). It normally involves attachment of yeast cells to, or location within, an insoluble support material by adsorption, covalent binding, entrapment, encapsulation or cross-linking (Gordon *et al.*, 2002). Among the different immobilization techniques, entrapment of microbial cell with the polymeric matrixes such as calcium alginate, gelatin, agar, k-carrageenan, etc or within some materials such as sponge, silicon carbide, polyurethane foam or chitosan has been widely studied (Razmovski *et al.*, 2011).

Silk fibroin (SF) is the typical natural macromolecule spun by *Bombyx mori* silkworm. It is an insoluble protein containing up to 90 % of the amino acids, like glycine (Gly), alanine (Ala), and serine (Ser). SF has been widely used as

biotechnology and biomedical materials because of its unique properties including good biocompatibility, good oxygen and water vapor permeability, biodegradability, minimal inflammatory reaction and non-toxicity (Um *et al.*, 2001). SF can be prepared for different morphologies such as particles, fibers, films, sponges, hydrogels and scaffolds (Vepari *et al.*, 2007). There are several fillers which may be mixed with SF in order to improve its mechanical properties and other properties. Cellulose whiskers (CLWs) are nanofiller extracted from plants. They can give reinforcement, tensile strength, Young's modulus and other good properties to composite.

The overall objective of this study is to develop a new carrier for yeast cells immobilization in order to use in continuous ethanol production. This carrier was prepared by fabricating SF/CLWs bionanocomposite sponges by using freeze drying technique. Furthermore, this study was considered the effect of SF-to-CLWs blended ratio on the chemical structure and morphology of bionanocomposite sponge. The carrier potential was evaluated by using in continuous ethanol fermentation in terms of % sugar consumption, residual sugar, ethanol production, ethanol yield and volumetric ethanol productivity that obtained from fermentation.

4.3 Experimental

4.3.1 Materials

The *Bombyx mori* silkworm cocoons were provided from the Queen Sirikit Department of Sericulture in Thailand. The *Musa sapientum* Linn banana rachises were obtained from local banana farm in Trang province, Thailand. *Saccharomyces cerevisiae burgundy* KY 11 yeast cell was purchased from Institute of Food Research and Product Development (IFRPD), Kasetsart University in the form of fresh yeast. Analytical grade of sodium hydroxide (NaOH) and sodium carbonate (Na_2CO_3) pellets were purchased from RANKEM. Calcium chloride dihydrate ($\text{CaCl}_2 \cdot 2\text{H}_2\text{O}$), analytical grade, was purchased from Analar[®]. D-glucose anhydrous, bacteriological peptone, and yeast extract powder were purchased from UNIVAR, CONDA, and Himedia, respectively. Analytical grade of ammonium sulfate ($(\text{NH}_4)_2\text{SO}_4$) was purchased from LOBA Chemie. Analytical grade of potassium dihydrogen phosphate (KH_2PO_4) was purchased from RANKEM. Hydrogen peroxide (H_2O_2) was purchased from Fisher Scientific Co., Ltd. 98 % of sulfuric acid (H_2SO_4) was purchased from J.T. Baker, Thailand. Methanol (CH_3OH) and ethanol ($\text{C}_2\text{H}_5\text{OH}$) (99.5 % purity), analytical grade, were purchased from RCI Labscan., Ltd. Both sodium potassium tartrate ($\text{KNaC}_4\text{H}_4\text{O}_6 \cdot 4\text{H}_2\text{O}$) and 3,5-dinitrosalicylic acid (DNS) were purchased from Sigma Aldrich.

4.3.2 Preparation of SF Solution

B. mori silk cocoons were cut into small pieces, washed by water, and dried in oven at 40 °C overnight. Then boil the silk cocoons in 0.05 % (w/v) Na_2CO_3 solution for 15 minutes (repeated for 2 times), wash them with boiled water and distilled water in order to obtain degummed silk. The degummed silk was dried in an oven at 40 °C overnight. A polar solvent system containing CaCl_2 , ethanol, and water at a CaCl_2 :ethanol:water molar ratio of 1:2:8 was prepared to dissolve the degummed silk. Then the silk fibroin solution was dialyzed in distilled water until negative test of AgNO_3 was found and followed by centrifuged at 10,000 rpm for 10 minutes. The SF solution was kept at 4 °C until use.

4.3.3 Preparation of CLWs

M. sapientum Linn banana rachis was cut into many small pieces about 15 mm to 20 mm of length and dried in oven at 40 °C overnight. The dried small banana rachis pieces were soaked in 4 % (w/v) NaOH at 80 °C for 2 hours to remove non-cellulosic materials to increase susceptibility to its hydrolysis and then thoroughly rinsed with distilled water. Then the banana rachises were bleached by treating with 5% (w/v) H₂O₂ solution at 70 °C for 2 hours. This step removed most of the residual lignin and protein. The bleached banana rachis fibers were hydrolyzed by 65% (w/v) H₂SO₄ at 60 °C for 4 hours under vigorous stirring. After that, CLWs were diluted with distilled water, centrifuged at 10,000 rpm for 10 minutes for three times and dialyzed until neutral.

4.3.4 Preparation of SF/CLWs Bionanocomposite Sponge

The SF solution was diluted with distilled water to get a concentration at 2% (w/v). The CLWs suspension was diluted to be 1% (w/v) and ultrasonicated for 15 minutes before adding into the SF solution at five different CLWs contents (10%, 20%, 30%, 40% and 50% based on weight ratio) with slow mechanical stirring. Then the mixture was stirred for 10 minutes and 1 ml of the mixture was pipetted to each well of COSTAR[®] 24-multi-wells culture plate and freeze dried at -40°C overnight.

4.3.5 Methanol Treatment of SF/CLWs Bionanocomposite Sponge

The SF and SF/CLWs bionanocomposite sponge were immersed in 90% (v/v) methanol solution for 10 minutes. And then the methanol-treated sponges were washed with an excessive amount of distilled water and dried by freeze drying at -40 °C for 24 hours.

4.3.6 Inoculums Preparation

To prepare an inoculum, 1 loop of yeast cell was added into a test tube containing 10 ml of Yeast Peptone Dextrose (YPD) broth growth medium consisting of D-glucose, peptone, and yeast extract at a concentration of 20 g·l⁻¹, 20 g·l⁻¹, and 10

$\text{g}\cdot\text{l}^{-1}$, respectively. The yeast culture was incubated in a shaking incubator at 150 rpm and 30 °C for 16 hours. Yeast cell concentration more than 10^8 cells·ml⁻¹ was obtained for using in the cell immobilization process.

4.3.7 Yeast Cells Immobilization

The methanol-treated SF/CLWs bionanocomposite sponge and 100 mL of YPD broth were autoclaved at 121 °C for 15 minutes. The sterilized sponges were immersed in the sterilized medium for 10 minutes. After that the inoculum yeast cells suspension were added to the sterilized medium. Then it was incubated in a shaking incubator at 150 rpm and 30 °C for 48 hours. After yeast cells were immobilized in the methanol-treated SF/CLWs bionanocomposite sponge, sponges were freeze dried at -40 °C overnight.

4.3.8 Continuous Ethanol Fermentation

The column containing the immobilized yeast cells was a tubular column that its inner diameter and height were about 3 and 40 cm, respectively. A tubular column was wrapped by jacket column in order to control the temperature within column (30 °C) during fermentation. The cooling bath circulator was used to control water temperature flowed within jacket column. The fresh nutrient medium was fed to the bottom of column and the effluent from column after fermentation was collected at the top of column. Both flow rate of feed in and feed out of medium in column were controlled by two peristaltic pumps. The 120 pieces of SF/CLWs bionanocomposite sponge containing yeast cells were contained in the column. The system was precultured and revitalized by feeding the medium at 0.6 ml/min of flow rate consisting of (in g/l): D-glucose, 20; peptone, 20; yeast extract, 10; (NH₄)₂SO₄, 1; KH₂PO₄, 1 at 30 °C for 24 hours. The working volume and height of the column were 247.30 ml and 35 cm, respectively.

The flow rates for the feed into the column with hydraulic retention time (H) 6.87, 5.15 and 4.12 hr were 0.6, 0.8, 1.0 ml/min, respectively. At the hydraulic retention time (H) 6.87, 5.15 and 4.12 hr corresponded to 0.15, 0.20 and 0.25 hr⁻¹ of dilution rate ($D=1/H$). The concentrations of 100, 150 and 200 g/l D-

glucose were used to be carbon sources for continuous ethanol fermentation. Furthermore, the feeding medium comprised of (in g/l): peptone, 20; yeast extract, 10; $(\text{NH}_4)_2\text{SO}_4$, 1; KH_2PO_4 , 1. The effluent from column was collected every three hours. The effluent sample was centrifuged at 10,000 rpm at 4°C for 10 minutes to remove cell pellets. The clear supernatant was determined the residual sugar concentration and ethanol content by DNS method and gas chromatography (GC), respectively.

4.3.9 Analytical Methods and Measurements

The chemical structure of SF, CLWs, and SF/CLWs bionanocomposite sponges were characterized by a Thermo Nicolet Nexus 671 FTIR spectrophotometer. The spectra were collected at a resolution of 4 cm^{-1} and 64 scans from 4000 cm^{-1} to 400 cm^{-1} of the wavenumber.

The TEM image of cellulose whiskers were detected by a JEOL JEM 2100 TEM microscope at an operating voltage of 200 kV. Samples for TEM observation were prepared by staining the diluted cellulose whiskers suspension with 1 % uranyl acetate aqueous solution. The sample was dropped on a carbon-coated copper grid and air-dried.

Both surface and cross-section morphology of the sponges were observed by a HITACHI S4800 FE-SEM microscope at an operating voltage of 2 kV. The sponges were coated with platinum by using a sputtering equipment operated for 200 seconds before the SEM observation.

The compression test was achieved at crosshead speed 1 mm/minute at room temperature. The compressive modulus of SF/CLWs bionanocomposite sponge was reported.

The number of yeast cells was counted directly under an Olympus CX31 OM microscope by the cell pellets resuspended in a 0.85 % NaCl solution before dropped to a Neubauer Precicolor HBG hemacytometer counting chamber.

An Tecant Infinite® 200 PRO UV-Vis spectrophotometer was used to analyze the utilization of reducing sugar by yeast cells during continuous ethanol fermentation process. The DNS method (Miller, 1959) based on the precipitation of residual sugar was used in order to determine the utilization of reducing sugar during

fermentation process. At a wavelength of 575 nm, the color intensities in terms of absorbance were measured. The sugar concentration was then determined from the D-glucose standard curve that was prepared in the concentration range of 0.2 to 1.0 (g/l).

A Shimazu GC-7AG instrument equipped with a flame ionization (FID) detector was used to determine ethanol concentration. A steel gas chromatograph column packed with Porapak Q was used. Temperature of the column and injector were fixed constant at 170 °C and 220 °C, respectively. Nitrogen (N₂) gas with the flow rate of 45 ml min⁻¹ was used as a carrier gas. Peak areas of the GC chromatograms of ethanol were compared with peak areas of the ethanol standard that was prepared in the concentration range of 0.01 to 15 (%v/v). Then ethanol concentration in the test sample was calculated.

Non-methanol and methanol-treated SF/CLWs bionanocomposite sponge were immersed in distilled water and incubated at 30 °C 150 rpm. The stability of bionanocomposite sponges in water was identified at various times (16, 24, 48, 72 hours). Weight loss (%) was calculated from this equation:

$$\% \text{ weight loss} = (W_i - W_f) / W_i \times 100$$

W_i : Initial dry weight of bionanocomposite sponge

W_f : Final dry weight of bionanocomposite sponge

The volume of the SF/CLWs bionanocomposite sponge before and after methanol treatment was calculated to identify the shrinkage (%) of bionanocomposite sponges after methanol treatment. Shrinkage (%) was calculated from this equation:

$$\text{Shrinkage (\%)} = (V_i - V_f) / V_i \times 100$$

V_i : The volume of the sponges before methanol treatment

V_f : The volume of the sponges after methanol treatment

A number of yeast cell contained SF/CLWs bionanocomposite sponge were counted. Then bionanocomposite sponge containing yeast cells were immersed in distilled water and incubated at 30°C 150 rpm for 24 hr in order to count a number of yeast cells which leaked out. The number of yeast cells in distilled water was

counted by Olympus CX31 OM microscope. Immobilization efficiency (%) and leakage (%) were calculated from these equations:

$$\text{Immobilization efficiency (\%)} = X_i/X_t \times 100$$

$$\text{Leakage (\%)} = X_f/X_t \times 100$$

X_i : Immobilized yeast cell concentration in sponges (cells/1 g of sponge) after immersing in distilled water for 24 hr.

X_f : Leaked free cell concentration in distilled water (cells/1 g of sponge) after immersing in distilled water for 24 hr.

X_t : Total initial immobilized yeast cell concentration in sponges (cells/1 g of sponge)

The sugar concentration was determined from the D-glucose standard curve that was prepared in the concentration range of 0.2 to 1.0 (g/l). The % sugar consumption was calculated by this equation:

$$\text{Sugar consumption (\%)} = (S_0 - S)/S_0 \times 100$$

S : Residual glucose concentration (g/l) at outlet

S_0 : Glucose concentration (g/l) in feed

Peak area of the GC chromatograms of the ethanol from fermentation was compared with peak areas of the ethanol standard prepared in the concentration range of 0.01 to 15 (%v/v).

Ethanol production was calculated by this equation:

$$\text{Ethanol production (g/l)} = P - P_0$$

P : Ethanol concentration (g/l) at outlet

P_0 : Initial ethanol concentration (g/l) = 0

Volumetric ethanol productivity (Q_p) was also calculated by this equation:

$$\text{Volumetric ethanol productivity (gl}^{-1}\text{hr}^{-1}\text{)} = P/H \text{ or } PD$$

P : Ethanol concentration (g/l) at outlet

H : Hydraulic retention time (hr)

D : Dilution rate (hr^{-1}) = $1/H$

Ethanol yield ($Y_{P/S}$) was determined from this equation:

$$\text{Ethanol yield} = P/S_0 - S$$

P : Ethanol concentration (g/l) at outlet

$S_0 - S$: Sugar consumption (g/l)

4.4 Results and Discussion

4.4.1 Characterization of Silk Fibroin (SF)

4.4.1.1 *Production Yield of SF Solution*

Degummed silk obtained from 10 g of silk cocoon was dissolved in 100 ml of solvent in order to get the production yield of SF solution. The solid content of SF solution was about 3.24% (w/v).



Figure 4.1 Appearance of silk fibroin solution.

Table 4.1 Production yield of silk fibroin solution

Material	Dry weight (g)
Silk cocoon	100
Degummed silk	72.70
Silk fibroin	61.40

4.4.1.2 *Chemical Analysis of SF and Methanol-treated SF*

Silk fibroin has major conformations in the solid state which are random coil (or silk I) and β -sheet (or silk II) structure. The silk I structure is the water-soluble state and is observed in vitro in aqueous conditions. On the other hand, the silk II structure of SF is insoluble in water and several solvents. So SF must be dissolved in the proper solvent system in order to disrupt the intermolecular hydrogen bond of beta sheet structure and still has random coil structure before preparing SF-based material. The obtained SF solution is random coil structure that

is called “regenerated SF”. In this experiment, regenerated SF was fabricated to be sponge by freeze dried technique. Figure 4.2 shows FTIR spectrum of SF sponge. The chemical structure of SF sponge was detected. The FTIR spectrum of SF sponge showed absorption peaks at 1655 cm^{-1} (amide I, C=O stretching), 1542 cm^{-1} (amide II, N-H bending vibration). These peaks are associated with random coil conformation of SF (silk I) (Um *et al.*, 2001; She *et al.*, 2008; Srisuwan *et al.*, 2011). Nevertheless, SF sponge can be induced its beta-sheet structure by methanol treatment. Figure 4.3 shows FTIR spectrum of SF sponge that was treated by methanol. The peaks of amide I and amide II were shifted to 1630 and 1523 cm^{-1} , respectively. These peaks are attributed to a β -sheet structure of SF (silk II) (Wongpanit *et al.*, 2007; Srisuwan *et al.*, 2011).

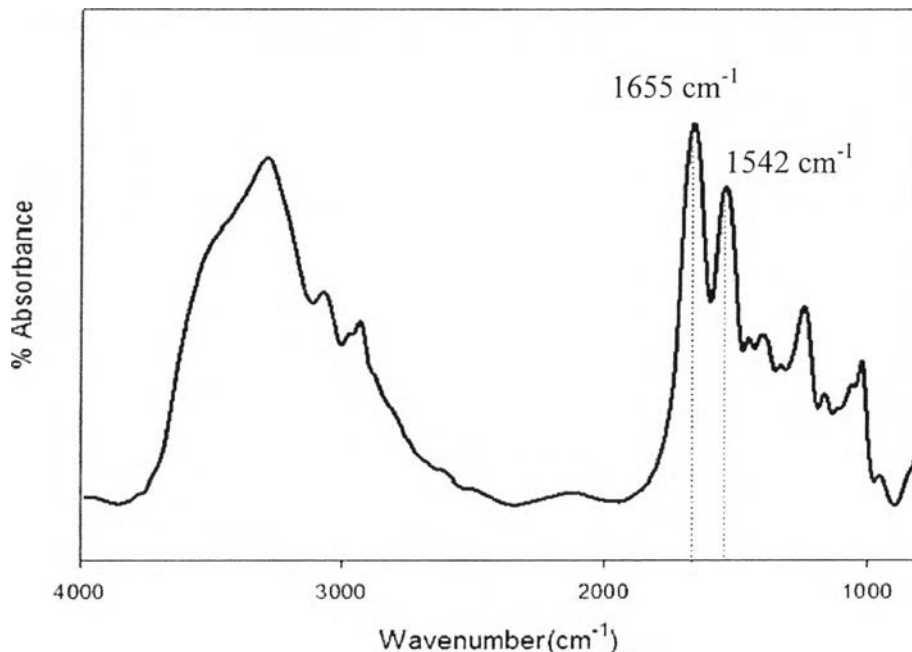


Figure 4.2 FTIR spectrum of SF sponge.

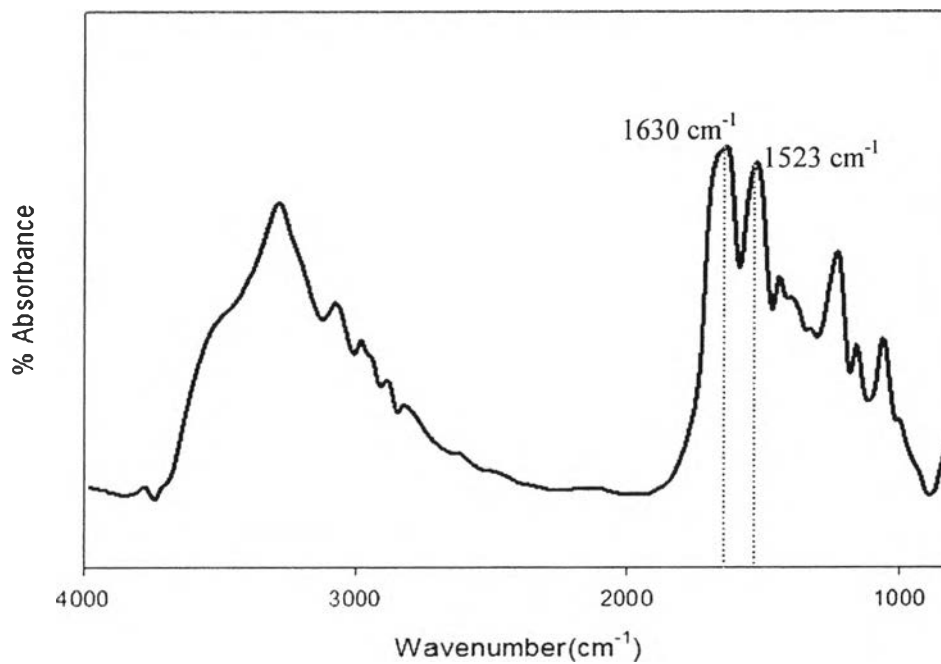


Figure 4.3 FTIR spectrum of methanol-treated SF sponge.

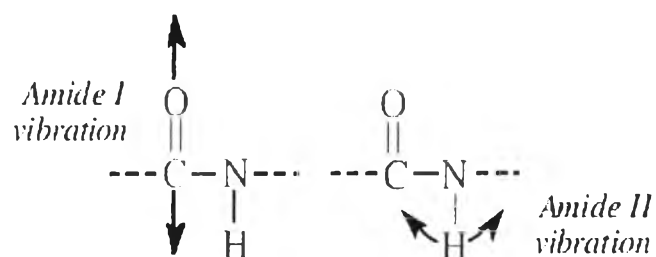


Figure 4.4 Chemical structure of silk fibroin.

4.4.2 Characterization of Cellulose Whiskers (CLWs)

4.4.2.1 *Production Yield of CLWs Suspension*

The production yield of CLWs suspension was obtained from 7 g of small pieces of dried banana rachis. The solid content of CLWs suspension after acid hydrolysis was about 1.28% (w/v).



Figure 4.5 Appearance of cellulose whiskers suspension.

Table 4.2 Production yield of CLWs suspension

Material/ Process	Dry weight (g)
Banana rachis	100
Immersed in 4% (w/v) NaOH	46.57
Bleaching step in 5% (w/v) H ₂ O ₂	25.57
Hydrolysis by 65% (w/v) H ₂ SO ₄	20.89

4.4.2.2 Morphological Analysis of CLWs

Figure 4.6 showed the morphology of CLWs extracted from banana rachis. The treatment under sulfuric acid hydrolysis resulted in removing the amorphous region of cellulosic microfibrils and remaining only crystalline region. Furthermore, the treatment also reduced the size of the fibers from the micron to the nanometer scale (Samir *et al.*, 2005). The diameter (D) and length (L) distribution of 100 samples of CLWs derived from banana rachis were shown in Figure 4.7. The average diameter and length of the CLWs were displayed to be 10.28 nm and 0.71 μm , respectively. The aspect ratio (L/D) is one of the most important parameters to indicate reinforcing capability of the CLWs. The aspect ratio of CLWs extracted from banana rachis was about 68.74.

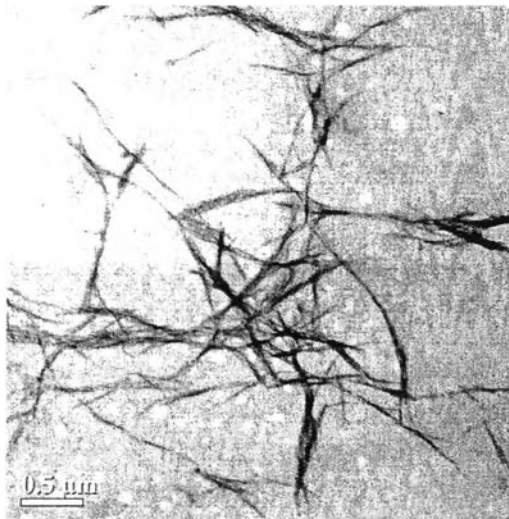


Figure 4.6 TEM image of cellulose whiskers suspension.

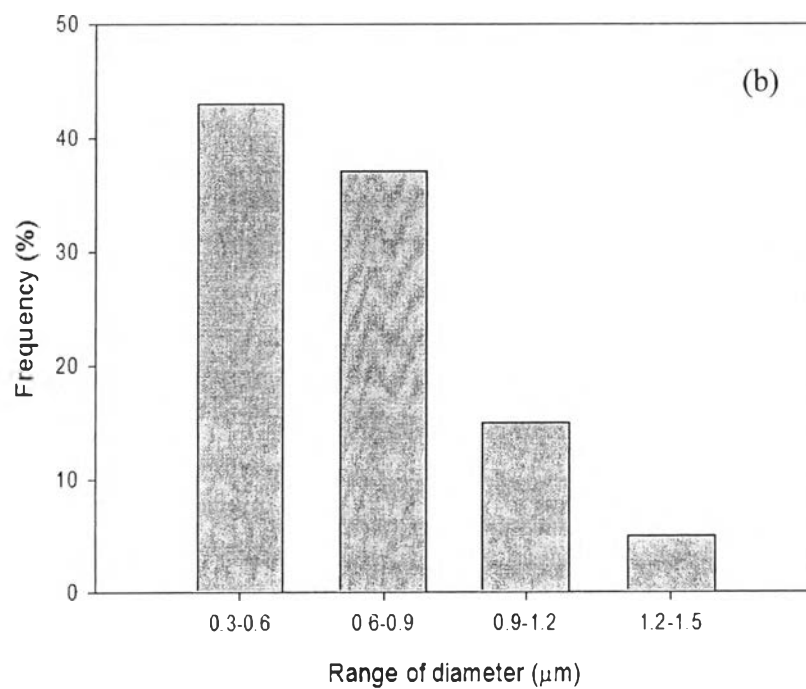
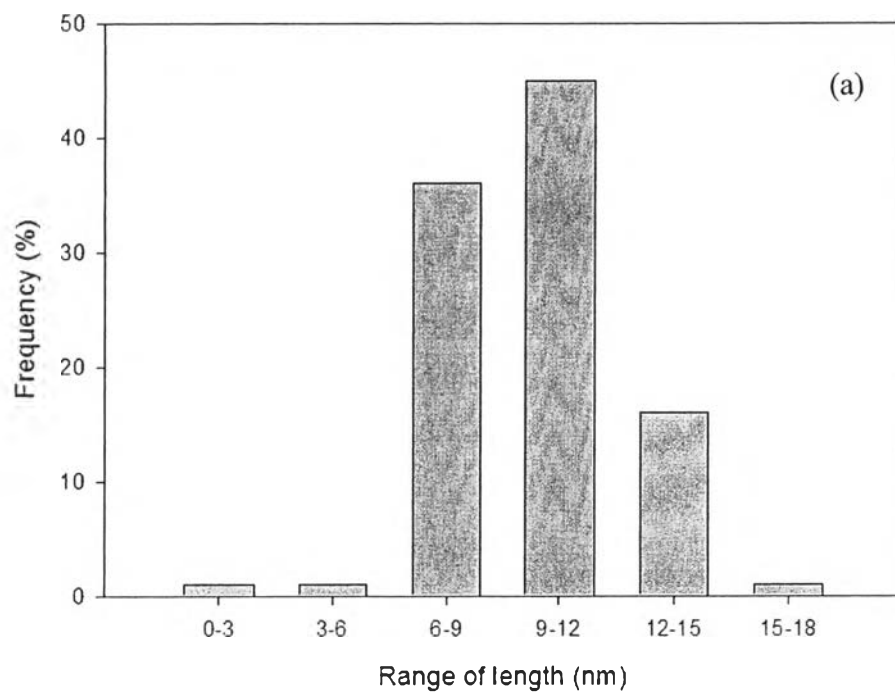


Figure 4.7 (a) The diameter distribution and (b) length distribution of CLWs derived from banana rachis.

4.4.2.3 Chemical Analysis of CLWs Suspension

The chemical structure of cellulose whiskers (CLWs) was assigned by FTIR spectroscopy as shown in Figure 4.8. The FTIR characteristic peaks were shown in Table 4.3. Native cellulose which was not treated by chemical has abundance of hemicellulose and lignin components. On the other hand, CLWs which were treated by NaOH, H₂O₂ and H₂SO₄, respectively has less hemicellulose and lignin. Constituents like pectins and hemicelluloses were hydrolyzed by the action of alkaline solutions (NaOH). Lignin was removed during additional steps using hydrogen peroxide (H₂O₂). This step is called “bleaching step”. The acid hydrolysis treatment was conducted on the cellulose fiber after alkaline treatment and bleaching in order to obtain cellulose nanocrystals (or CLWs) (Zuluaga *et al.*, 2009; Nurain *et al.*, 2012). The absorption peak located around 1633 cm⁻¹ is representative of C=C aromatic of lignin. The peak at 1429 and 1320 cm⁻¹ are assigned to C-H deformation and C-H₂ wag of cellulose, respectively. The absorption peak at 1163 cm⁻¹ was attributed to C-O-C asymmetric stretching of cellulose. The C-O stretching of cellulose was appeared at 1061 cm⁻¹ (Zuluaga *et al.*, 2007; Zuluaga *et al.*, 2009; Rosa *et al.*, 2010).

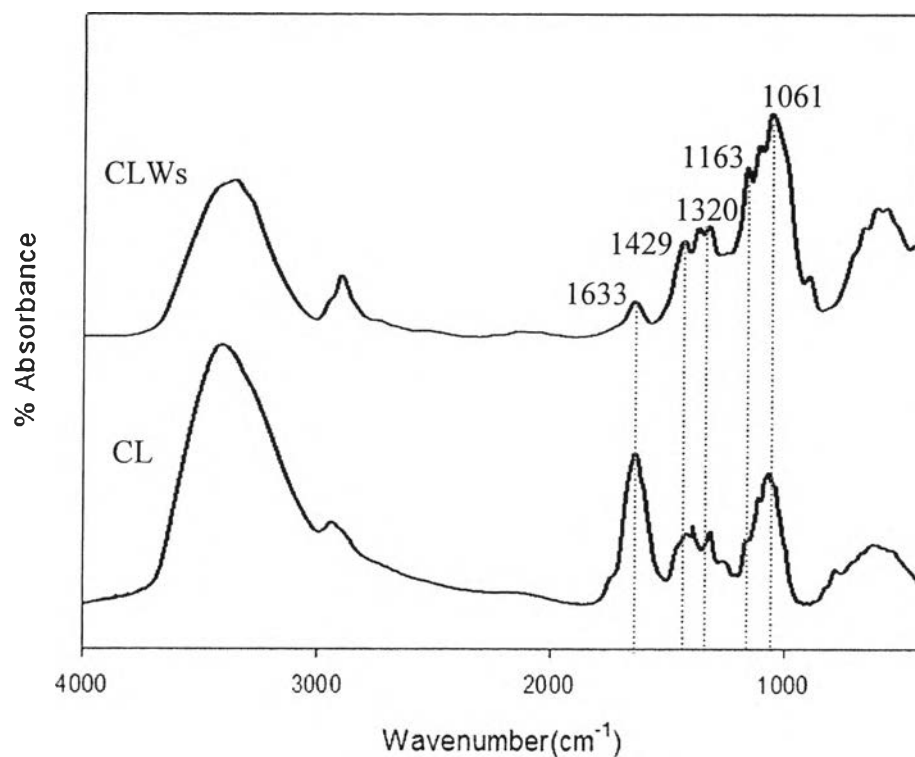


Figure 4.8 FTIR spectra of native cellulose (CL) and CLWs.

Table 4.3 The main functional groups of CLWs

Wavenumber (cm ⁻¹)	Peak assignments
1633	C=C aromatic of lignin
1429	C-H deformation of cellulose
1320	C-H ₂ wag of cellulose
1163	C-O-C asymmetric stretching of cellulose
1061	C-O stretching of cellulose

4.4.3 Characterization of SF/CLWs Bionanocomposite Sponge

4.4.3.1 *The SF/CLWs Bionanocomposite Sponge Codes at Various Weight Ratios of SF to CLWs*

Table 4.4 and 4.5 illustrated the non-methanol treated and the methanol-treated bionanocomposite sponge codes at various weight ratios of SF to CLWs, respectively.

Table 4.4 The non-methanol treated bionanocomposite sponge codes at various weight ratios of SF to CLWs

Bionanocomposite sponge codes	SF (wt%)	CLWs (wt%)
SF100	100	0
SF90	90	10
SF80	80	20
SF70	70	30
SF60	60	40
SF50	50	50

Table 4.5 The methanol-treated bionanocomposite sponge codes at various weight ratios of SF to CLWs

Bionanocomposite sponge codes	SF (wt%)	CLWs (wt%)
MSF100	100	0
MSF90	90	10
MSF80	80	20
MSF70	70	30
MSF60	60	40
MSF50	50	50

4.4.3.2 Morphological Analysis of SF/CLWs Bionanocomposite Sponge

Figure 4.9 and 4.10 were the SEM micrographs that illustrated the morphology of bionanocomposite sponges. The bionanocomposite sponges exhibited porous material with interconnected pores in order to allow the growth of yeast cells and the culture medium or nutrient to penetrate into yeast cells entrapped and attached inside the sponges. The pore size of sponges depended on a freeze-drying and a content of CLWs in sponges. Using the freeze-drying technique, the suspension of SF/CLWs bionanocomposite is frozen or solidified. The SF/CLWs bionanocomposite is localized during the nucleation of ice crystals. Sublimation of ice crystals brings about formation of a highly porous bionanocomposite sponges. Decreasing of nucleation rate or freezing rate in the freezing process leads to the larger ice crystals, so the sponges with a larger average pore diameter are obtained. Furthermore, the direction of heat transfer and speed of heat transfer affect the shape of crystal. The pore width of SF/CLWs bionanocomposite sponges increased with increasing weight ratio of CLWs in sponges (see Table 4.6). Increasing of CLWs content causes impeding the direction and speed of heat transfer of water molecule that effects slow *in situ* freezing rate, enlarging the ice particles, and finally bringing about the larger pore width of SF/CLWs bionanocomposite sponge (Fergal *et al.*, 2004).

Table 4.6 Average pore width of bionanocomposite sponge

Bionanocomposite sponge	Average pore width (μm)
MSF100	16.96 ± 5.05
MSF90	26.55 ± 8.26
MSF80	55.24 ± 13.43
MSF70	69.89 ± 12.25
MSF60	91.13 ± 20.61
MSF50	112.65 ± 24.66

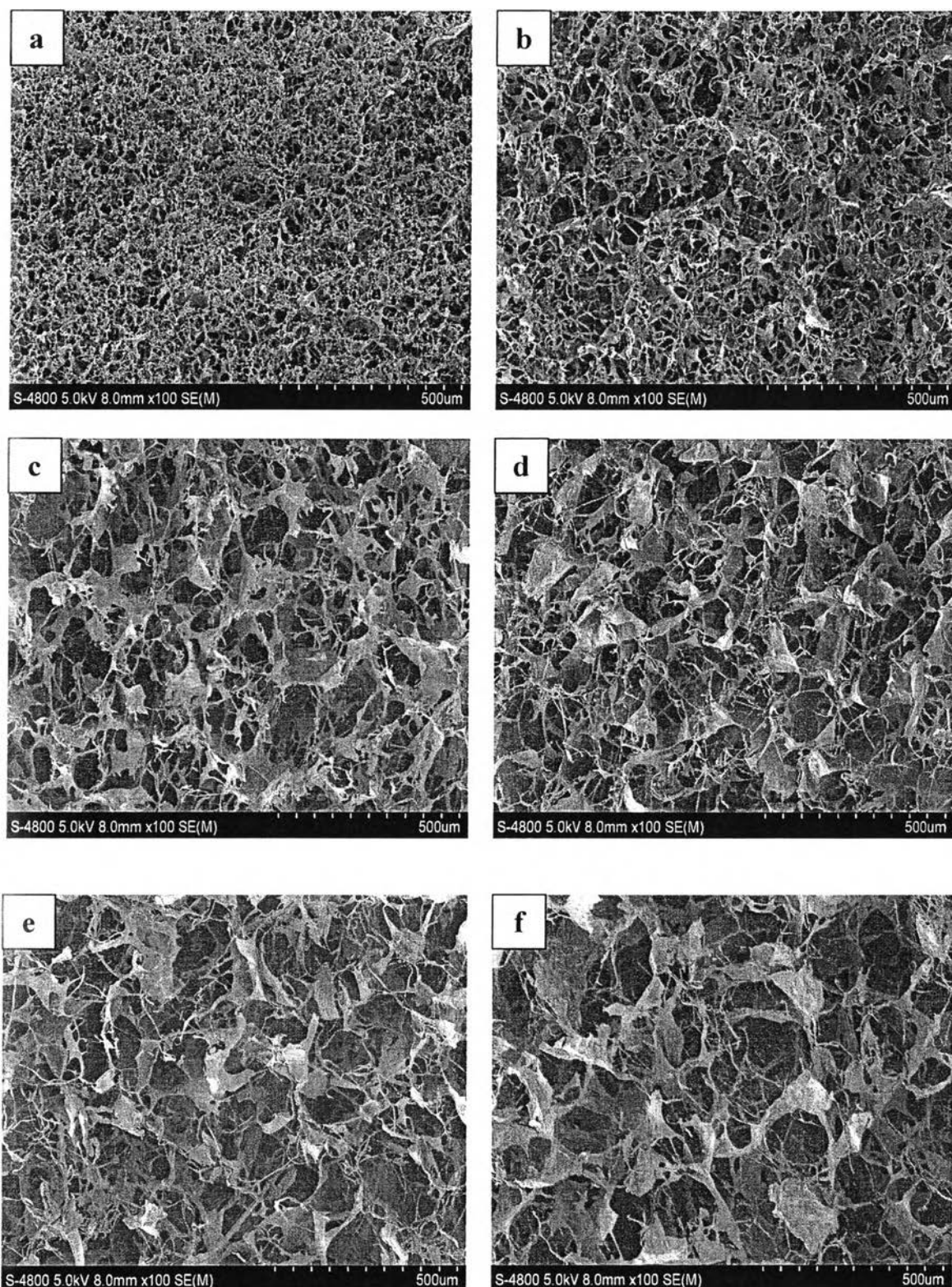


Figure 4.9 SEM images of surface of (a) methanol-treated SF sponge and (b), (c), (d), (e), (f) methanol-treated bionanocomposite sponges at SF/CLWs ratio of 90/10, 80/20, 70/30, 60/40 and 50/50, respectively.

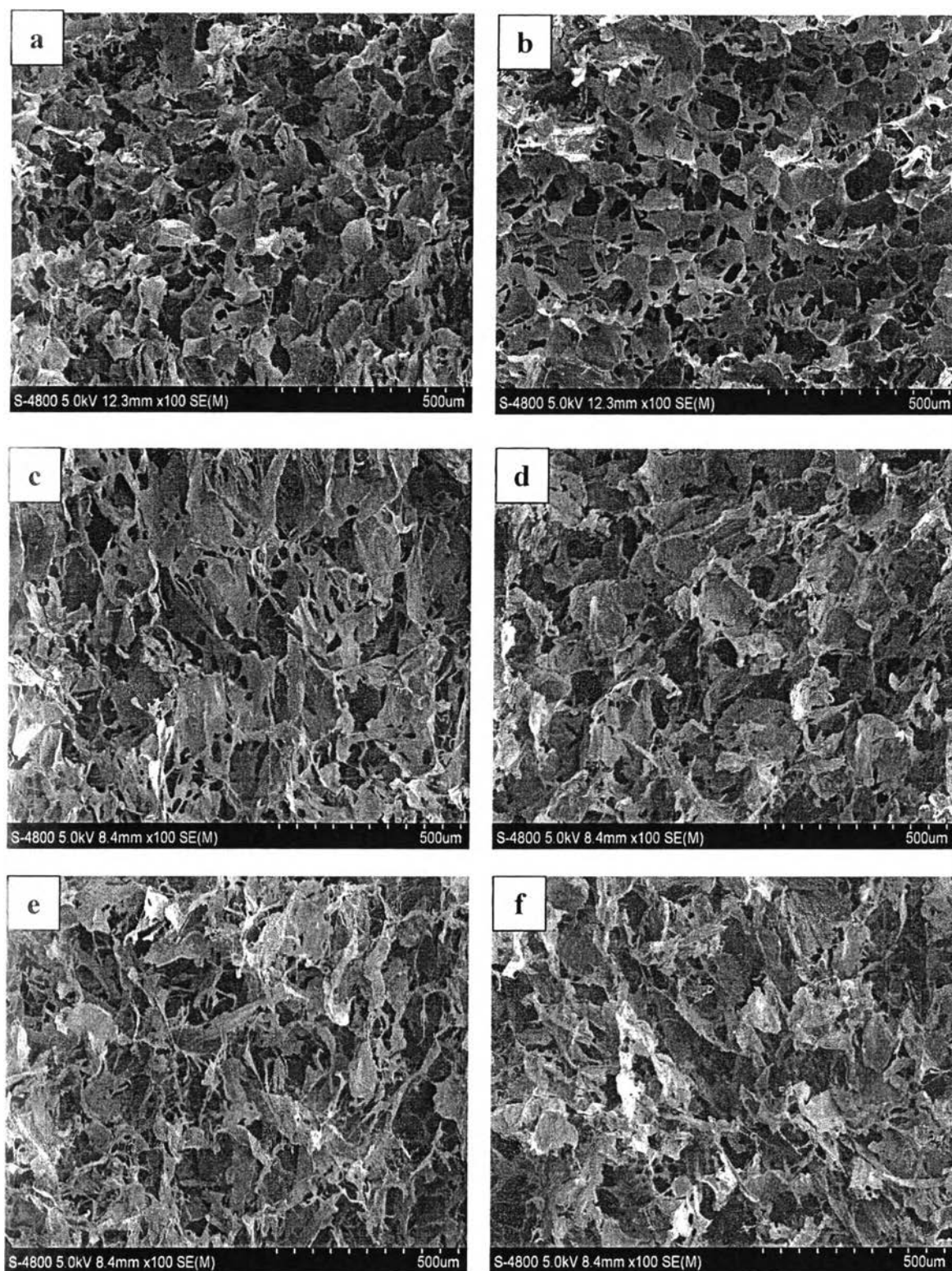


Figure 4.10 SEM images of cross sectional part of (a) methanol-treated SF sponge and (b), (c), (d), (e) and (f) methanol-treated bionanocomposite sponges at SF/CLW's ratio of 90/10, 80/20, 70/30, 60/40 and 50/50, respectively.

4.4.3.3 Chemical Analysis of Methanol-treated SF/CLWs Bionanocomposite Sponge

Figure 4.11 showed FTIR spectra of SF, CLWs and SF/CLWs bionanocomposite sponge at various ratios after methanol treatment. The FTIR characteristic peaks of methanol-treated SF/CLWs bionanocomposite sponge showed that absorption peaks of amide I and amide II were shifted to 1630 and 1523 cm^{-1} , respectively (Wongpanit *et al.*, 2007; Srisuwan *et al.*, 2011). The peaks were shifted because conformation of SF/CLWs bionanocomposite sponge was changed to be β -sheet structure after methanol treatment. The treatment in polar solvent, aqueous methanol, are highly effective in crystallization of SF (Park *et al.*, 2004). The methanol molecules can impede the hydrogen bond of random coil SF and induce the beta-sheet conformation. Furthermore, absorption peaks at 1633, 1429, 1320, 1163 and 1061 cm^{-1} which were representative of C=C aromatic of lignin, C-H deformation of cellulose and C-H₂ wag of cellulose, C-O-C asymmetric stretching of cellulose and C-O stretching of cellulose, respectively, were associated with the chemical structure of CLWs (Zuluaga *et al.*, 2007; Zuluaga *et al.*, 2009; Rosa *et al.*, 2010). The blending SF with CLWs also induces SF structure from random coil into β -sheet because of the surface of crystalline CLWs and hydrogen bonding between -OH of CLWs and -NH₂ and/or -OH of SF (Noshiki *et al.*, 2002; Shang *et al.*, 2011).

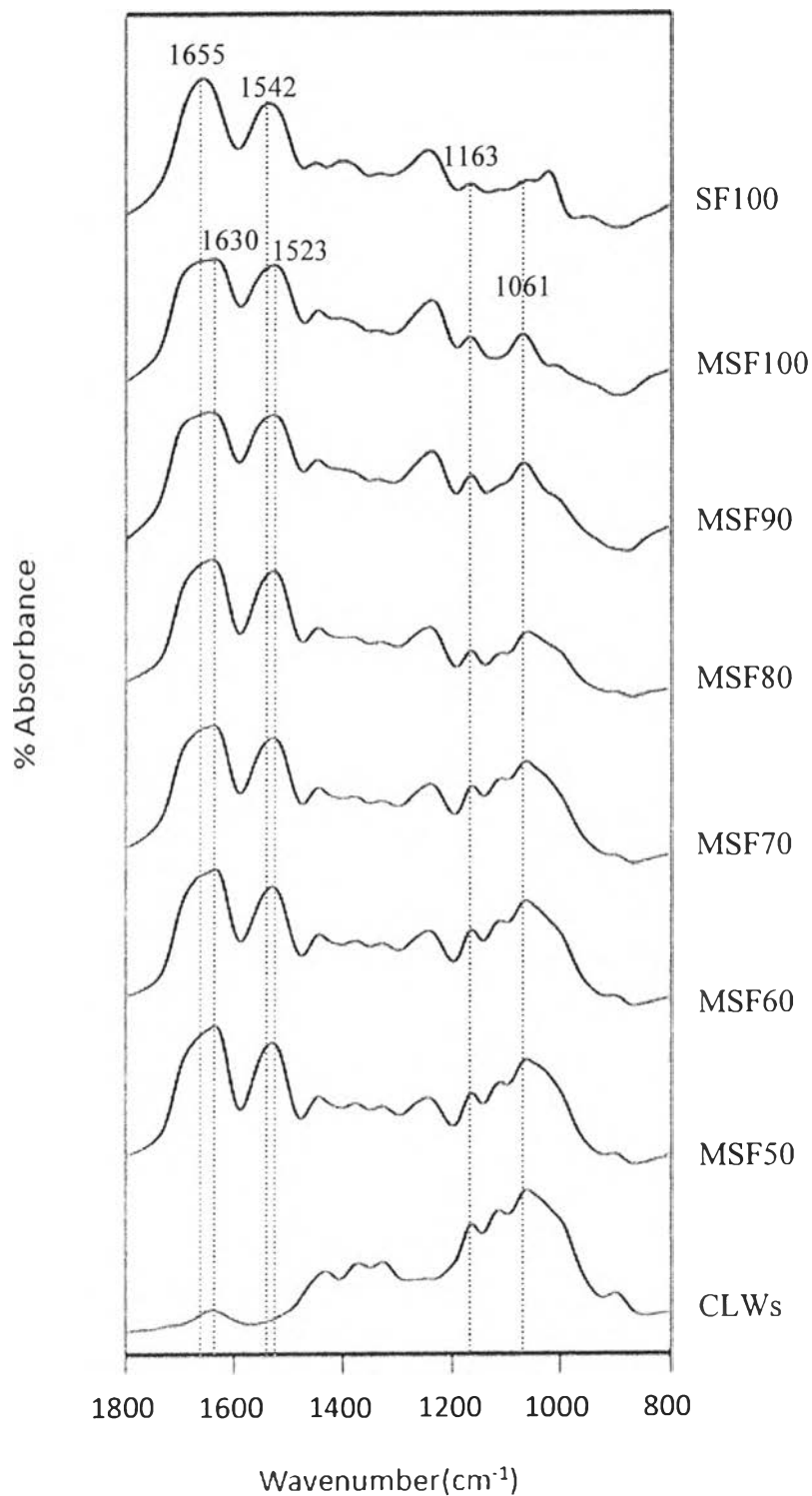


Figure 4.11 FTIR spectra of SF, CLWs and SF/CLWs bionanocomposite sponge at various ratios after methanol treatment.

4.4.3.4 Weight Loss of SF/CLWs Bionanocomposite Sponge

Figure 4.12 showed weight loss (%) of non-methanol treated SF/CLWs bionanocomposite sponges at various times (16, 24, 48, 72 hours). The %weight loss of bionanocomposite sponges increased when the immersion time in distilled water increased. And the %weight loss decreased with increasing weight ratio of CLWs in bionanocomposite sponges. Figure 4.13 showed weight loss (%) of methanol-treated bionanocomposite sponges in distilled water. Their %weight loss have the same trend as the %weight loss of non-methanol treated bionanocomposite sponges. However, the value of %weight loss of methanol-treated bionanocomposite sponges was less than the non-treated ones because of beta-sheet structure in methanol-treated bionanocomposite sponges. The silk I structure in SF is the water-soluble state and also known as random coil structure. The random coil structure could be induced to beta-sheet structure (or silk II) which is insoluble and stable in water by methanol treatment. Therefore, the better dimension stability in water of the methanol-treated bionanocomposite sponges resulted from the conformation transition from random coil to beta-sheet structure of SF. The beta-sheet structure in methanol-treated bionanocomposite sponges was confirmed by the characteristic peaks in FTIR of beta-sheet conformation. The methanol-treated bionanocomposite sponges of MSF50 gave the most excellent water stability in this experiment.

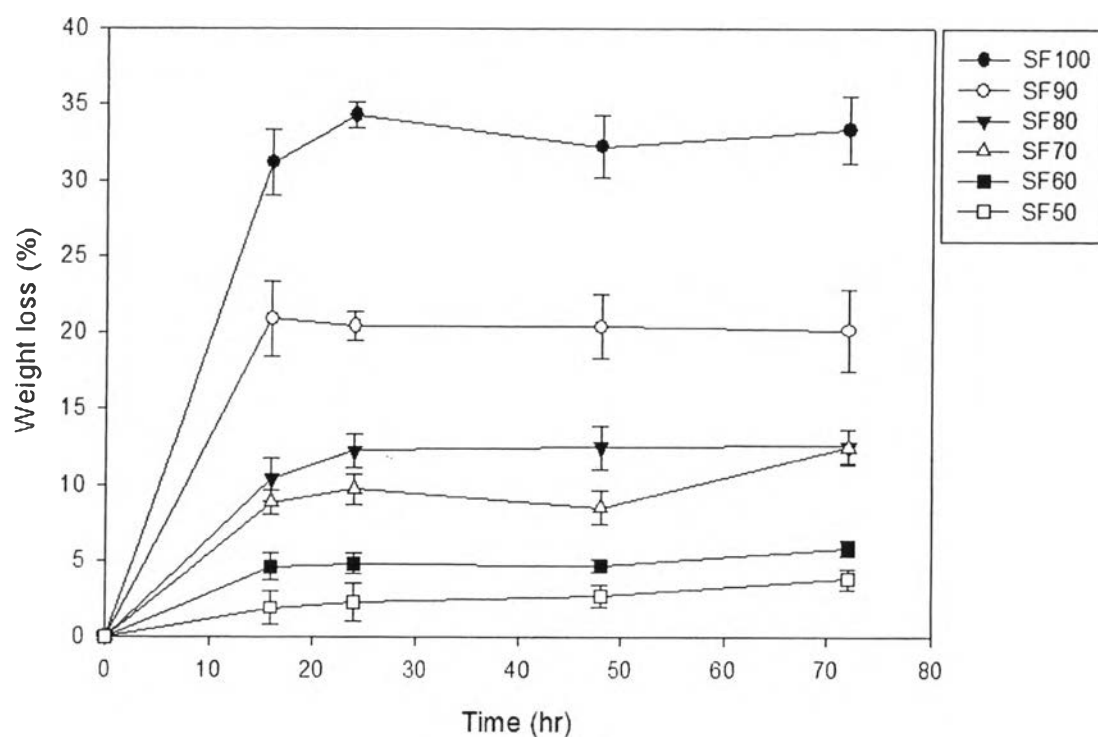


Figure 4.12 Weight loss of non-methanol treated bionanocomposite sponges.

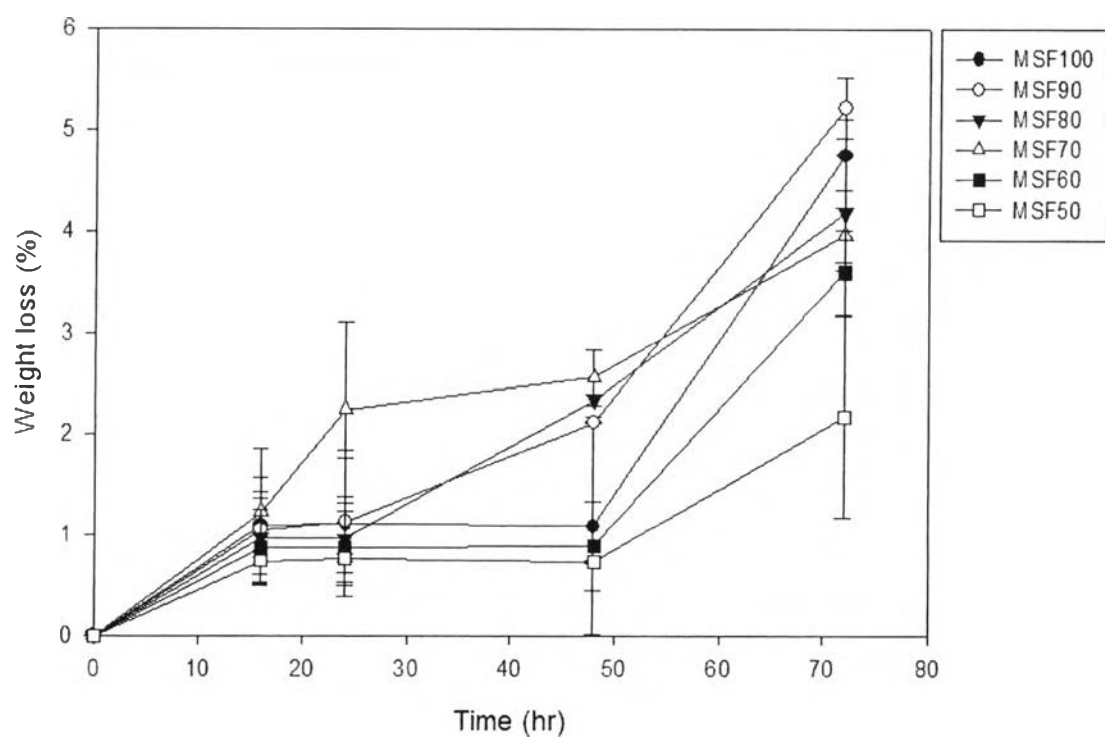


Figure 4.13 Weight loss of methanol-treated bionanocomposite sponges.

4.4.3.5 Shrinkage of SF/CLWs Bionanocomposite Sponge

Figure 4.14 illustrated shrinkage (%) of bionanocomposite sponges both with and without CLWs after methanol treatment. The change in volume of the bionanocomposite sponges before and after methanol treatment was measured in order to determine their dimensional stability. In general, the conformation transition of the porous material influences the shrinkage and poor dimensional stability. Methanol treatment of SF/CLWs bionanocomposite sponges induced the transition of random coil conformation to beta-sheet structure in SF, which resulted in the shrinkage of materials. However, it was found that the % shrinkage of the bionanocomposite sponges could be decreased with increasing CLWs ratios. It referred that CLWs can improve dimensional stability of bionanocomposite sponge.

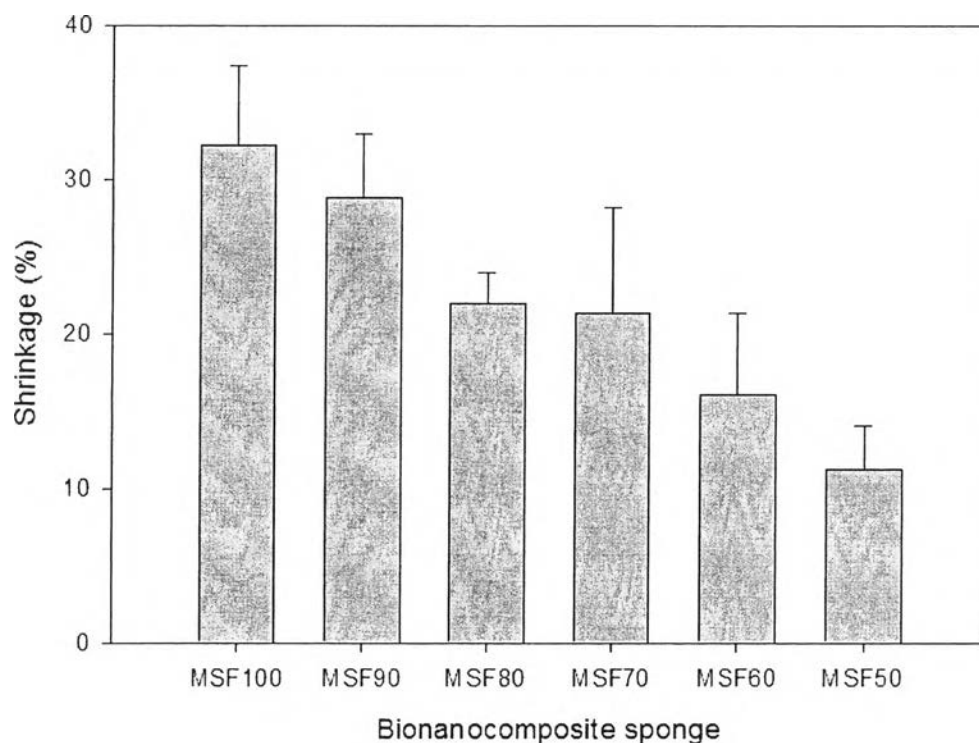


Figure 4.14 Shrinkage (%) of bionanocomposite sponges at various ratios after methanol treatment.

4.4.3.6 *The Compression Modulus of Methanol-treated SF/CLWs Bionanocomposite Sponge*

Figure 4.15 showed information of the compression modulus methanol-treated SF/CLWs bionanocomposite sponge. The compression modulus of bionanocomposite sponge increased with increasing CLWs content and reached a maximum when the CLWs content was equal to 50% of weight ratio (MSF50). Shang *et al.*, (2011) studied mechanical properties of silk fibroin/cellulose (SF/CE) blend films and found that the elongation at break of the blend films displays the initial ascent trend when CE content increased to 50 wt% and then took a rapid drop for 75 wt% CE content due to bad compatibility between SF and CE. The blend film containing 50 wt% of cellulose had excellent compatibility between SF and CE, contributing to the higher elongation at break. To explain the increase of the compression modulus, the incorporation of CLWs to bionanocomposite sponges caused intermolecular hydrogen bond between –OH of CLWs and –NH₂ and/or –OH of SF (as shown in Figure 4.16) and induced beta-sheet conformation of SF. At 50% weight ratio of CLWs provided the strongest intermolecular interactions in matrix, causing the maximum the compression modulus.

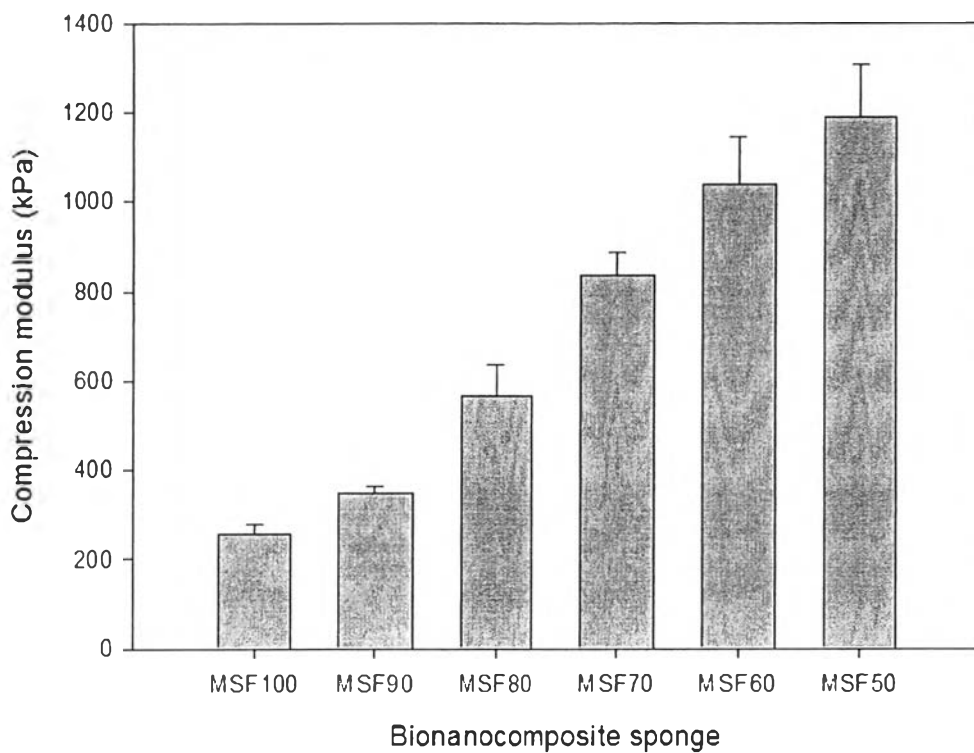


Figure 4.15 Compression modulus of methanol- treated bionanocomposite sponges.

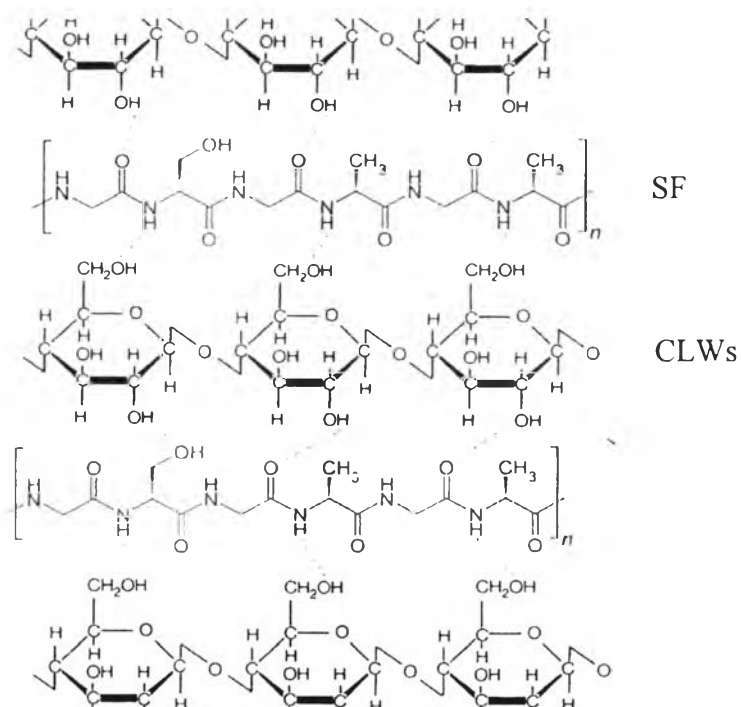


Figure 4.16 Possible intermolecular hydrogen bond between SF and CLWs.

4.4.3.7 Yeast Cell Immobilization and Yeast Cell Leakage in Methanol-treated SF/CLWs Bionanocomposite Sponge

Figure 4.17(a) and (b) illustrated a number of immobilized yeast cells and the %immobilization efficiency in the methanol-treated SF/CLWs bionanocomposite sponge at various weight ratios, respectively. The Neubauer Precicolor HBG hemacytometer counting chamber was used for counting yeast cells. A larger number of yeast cells were attached in bionanocomposite sponge which had higher CLWs content. The highest number of yeast cells were attached inside the bionanocomposite sponge containing 50% weight ratio of CLWs (MSF50) because MSF50 presented the largest pore sizes that allowed better yeast cell growth and penetration and better the culture medium or nutrient transfer into yeast cells entrapped and attached inside the sponges. Furthermore, CLWs had high surface area that provided surface for attachment of yeast cells. Figure 4.18 showed SEM images of a large number of yeast cells attached inside MSF50 bionanocomposite sponge.

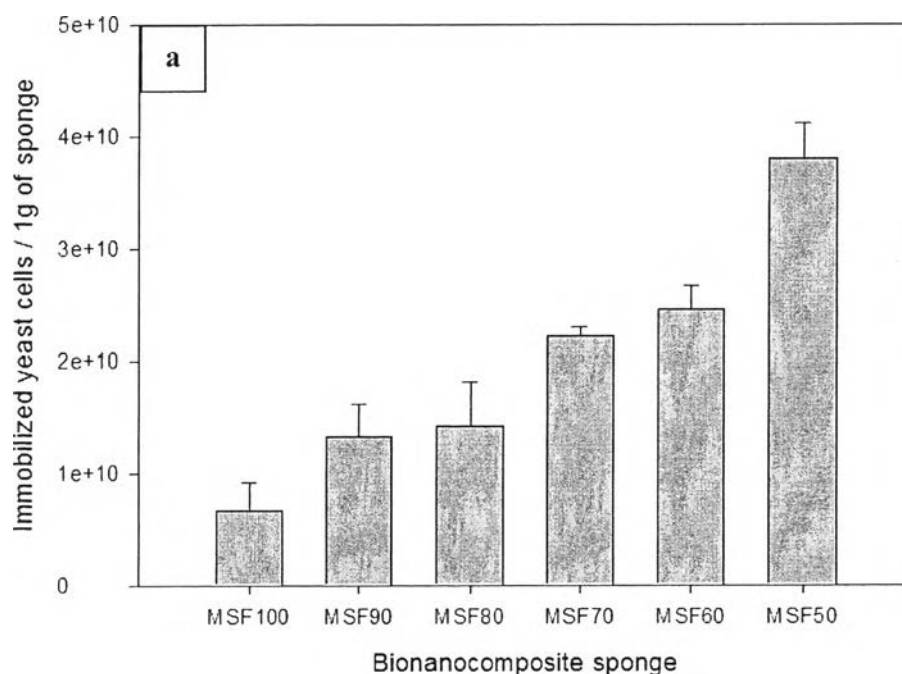


Figure 4.17 (a) A number of immobilized yeast cells in the methanol-treated SF/CLWs bionanocomposite sponge at various weight ratios.

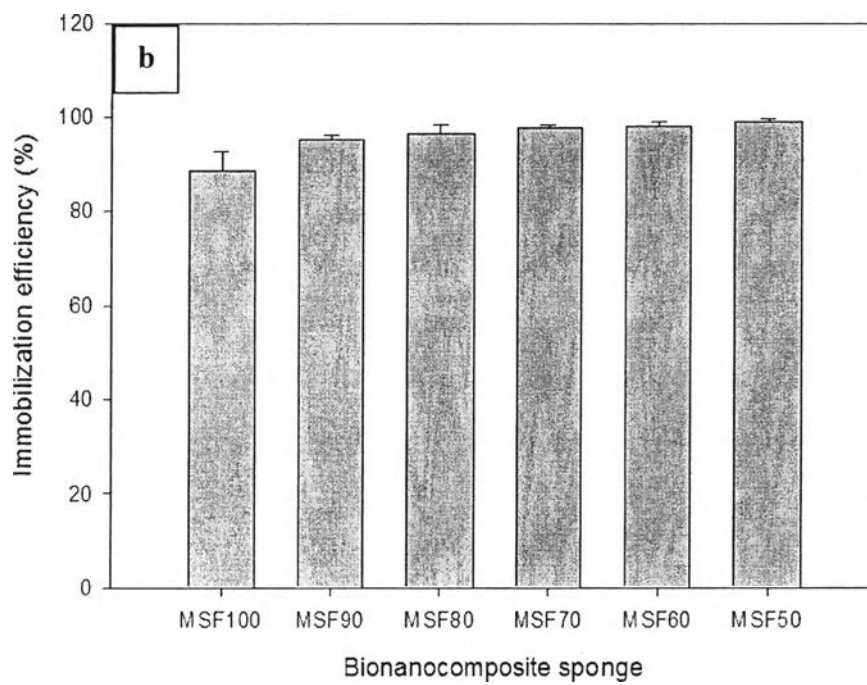


Figure 4.17 (b) The % immobilization efficiency in the methanol-treated SF/CLWs bionanocomposite sponge at various weight ratios.

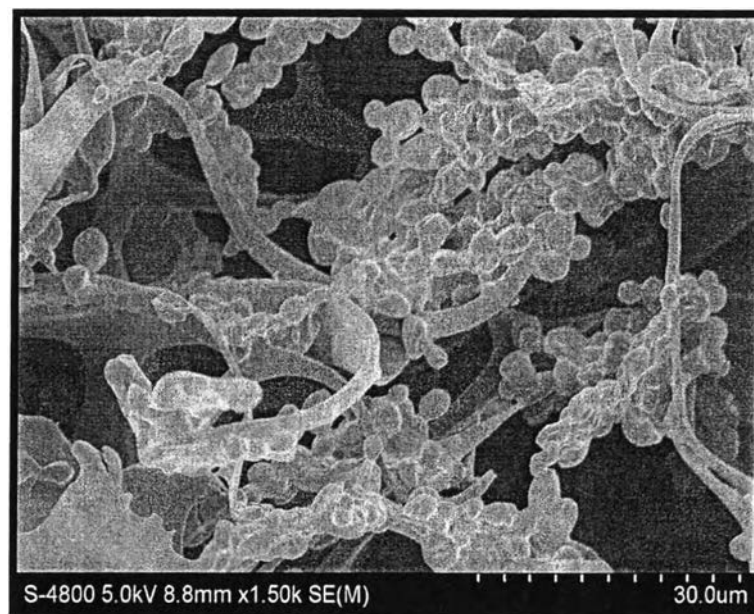
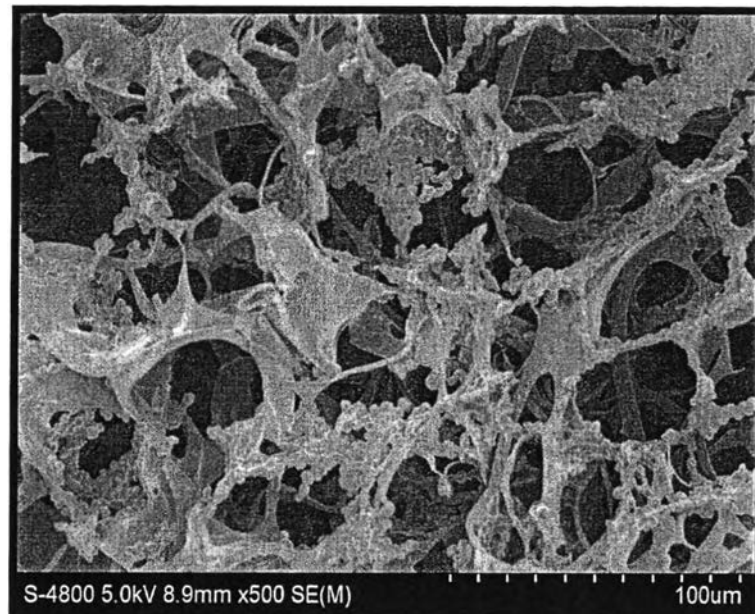


Figure 4.18 SEM images of a large number of yeast cells attached inside MSF50 bionanocomposite sponge.

A number of yeast cells which leaked from methanol-treated SF/CLWs bionanocomposite sponge and % yeast cells leakage were shown in Figure 4.19(a) and (b), respectively. The decrease of yeast cell leakage appeared in bionanocomposite sponge having higher CLWs content. With high CLWs content in bionanocomposite sponge, % weight loss of bionanocomposite sponge was low (as shown in Figure 4.13); therefore, the attached yeast cells on surface of bionanocomposite sponge less leaked.

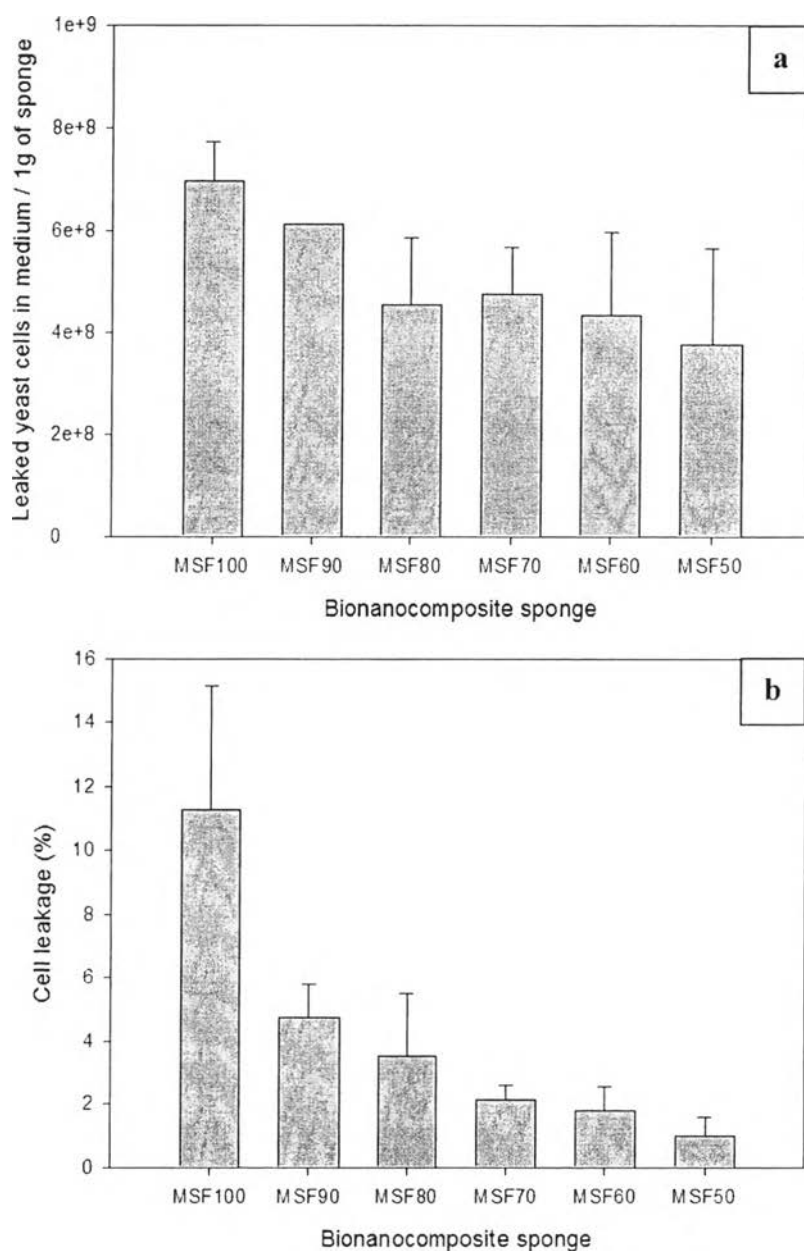


Figure 4.19 (a) A number of leaked yeast cells and (b) the % cell leakage from the methanol-treated SF/CLWs bionanocomposite sponge at various weight ratios.

4.4.4 Continuous Ethanol Fermentation

Continuous ethanol fermentation was carried out by using the column reactor (packed-bed reactor) containing the immobilized yeast cells within MSF50 bionanocomposite sponge. The MSF50 bionanocomposite sponge was chosen as a carrier for immobilization of yeast cell because MSF50 had highest pore size, water stability, dimensional stability, yeast cell density and lowest cell leakage. The continuous fermentation system was operated by the following operating condition: temperature at 30°C, pH at 4.5-5, feed sugar concentrations of 100, 150, and 200 g/l, dilution rate (D) of 0.15, 0.20 and 0.25 hr⁻¹ corresponded to 6.87, 5.15 and 4.12 hr of hydraulic retention time (H).

4.4.4.1 *Sugar Consumption and Ethanol Production*

Figure 4.20(a), (b), and (c) illustrated the effect of feed glucose concentration and dilution rate on the ethanol production, volumetric ethanol productivity (Q_p) and ethanol yield ($Y_{P/S}$), respectively. At a feed glucose concentration of 100, 150, 200 g/l and dilution rate 0.15 hr⁻¹, 41.31, 42.07, and 51.18 g/l of ethanol production with the volumetric ethanol productivity (Q_p) of 6.20, 6.31, and 7.68 g l⁻¹hr⁻¹ and the ethanol yield ($Y_{P/S}$) of 0.48, 0.38, and 0.41 were obtained respectively. At a feed glucose concentration of 100, 150, 200 g/l and dilution rate 0.20 hr⁻¹, 36.62, 40.45, and 46.90 g/l of ethanol production with the volumetric ethanol productivity (Q_p) of 7.32, 8.09, and 9.38 g l⁻¹hr⁻¹ and the ethanol yield ($Y_{P/S}$) of 0.44, 0.38, and 0.40 were gained respectively. Furthermore, at a feed glucose concentration of 100, 150, 200 g/l and dilution rate 0.25 hr⁻¹, 33.19, 34.44, and 42.22 g/l of ethanol production with the volumetric ethanol productivity (Q_p) of 8.30, 8.61, and 10.56 g l⁻¹hr⁻¹ and the ethanol yield ($Y_{P/S}$) of 0.40, 0.37, and 0.39 were gained respectively.

A value of % sugar consumption and residual sugar concentration were shown in Figure 4.21(a) and (b), respectively. A % sugar consumption of 86.90, 73.20, and 62.89% and a residual sugar concentration of 13.10, 40.20, and 74.21 g/l at the operating condition of a feed glucose concentration of 100, 150, 200 g/l and dilution rate 0.15 hr⁻¹ were obtained respectively. A % sugar consumption of 83.16, 70.61, and 59.32% and a residual sugar concentration of 16.84, 44.08, and 81.35 g/l at the operating condition of a feed glucose concentration

of 100, 150, 200 g/l and dilution rate 0.20 hr^{-1} were obtained respectively. A % sugar consumption of 82.11, 61.99, and 54.54% and a residual sugar concentration of 17.89, 57.01, and 90.92 g/l at the operating condition of a feed glucose concentration of 100, 150, 200 g/l and dilution rate 0.25 hr^{-1} were gained respectively.

Under continuous ethanol fermentation in packed-bed bioreactor, the maximum ethanol production of 51.18 g/l with the volumetric ethanol productivity of $7.68 \text{ g l}^{-1} \text{ hr}^{-1}$ was obtained at 0.15 hr^{-1} dilution rate and 200 g/l feed glucose concentration. All of information indicated that the ethanol production and volumetric ethanol productivity increased when the feed glucose concentration increased but the % sugar consumption decreased. The % sugar consumption of yeast cell in fermentation decreased when the feed glucose concentration increased because using high feed glucose concentration caused high ratio of glucose to yeast cell mass concentration or sugar uptake limit.

4.4.4.2 Effect of Dilution Rate on Continuous Ethanol Fermentation

The feed glucose concentration of 100, 150, and 200 g/l were passed through the column with different dilution rate varying at of 0.15, 0.20 and 0.25 hr^{-1} . The Figure 4.20(a) indicated that the ethanol production was decreased at high dilution rate because of less interaction time of glucose molecule with the immobilized yeast cells or low hydraulic retention time (H) that means decreasing in sugar consumption of yeast cell. On the other hand, Figure 4.20(b) shows that the volumetric ethanol productivity (Q_P) was increased when the dilution rate was increased from 0.15 to 0.25 hr^{-1} . The high dilution rate represented as high flow rate of ethanol production, so the amount of ethanol production per hour was high, which resulted in high the volumetric ethanol productivity (Q_P).

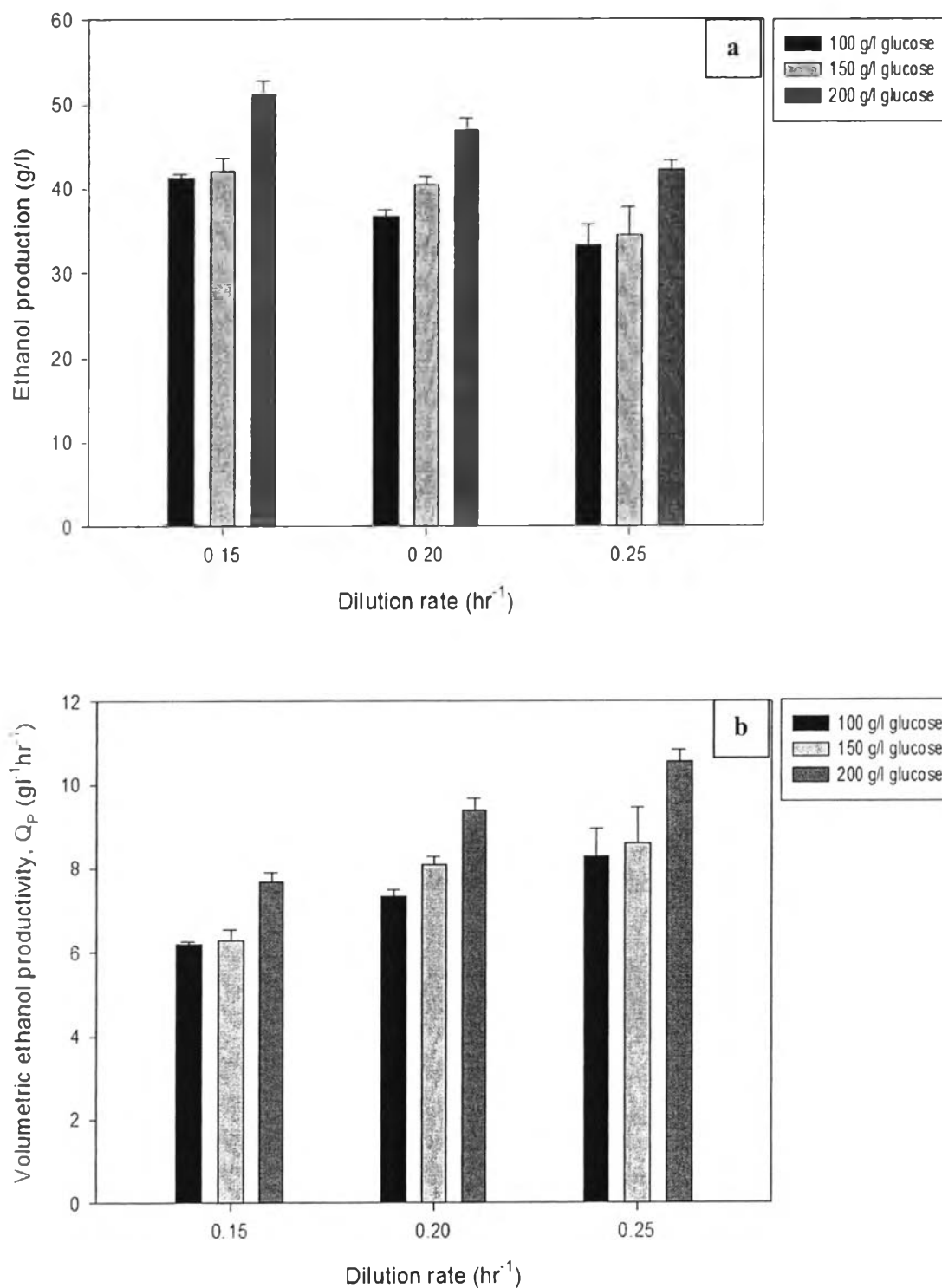
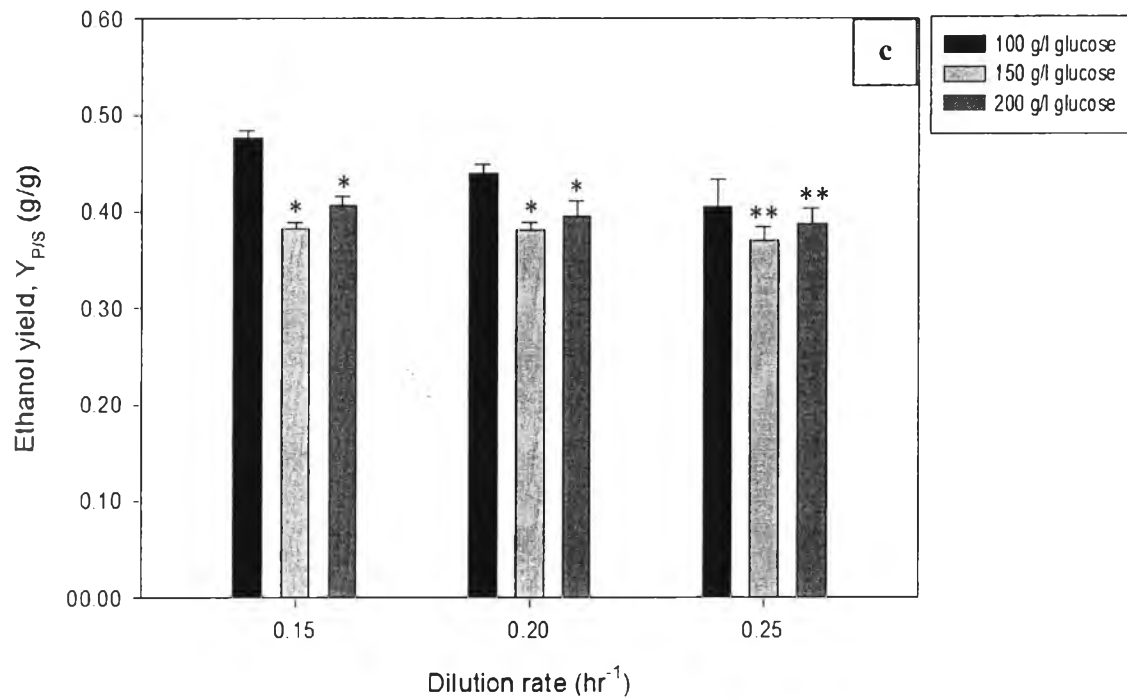


Figure 4.20 The effect of feed glucose concentration and dilution rate on (a) the ethanol production and (b) volumetric ethanol productivity (Q_p).



* represents statistically significant, $p < 0.01$

** represents not statistically significant, $p > 0.05$

; statistically significant against 100 g/l of feed glucose concentration.

Figure 4.20 (c) The effect of feed glucose concentration and dilution rate on ethanol yield ($Y_{P/S}$).

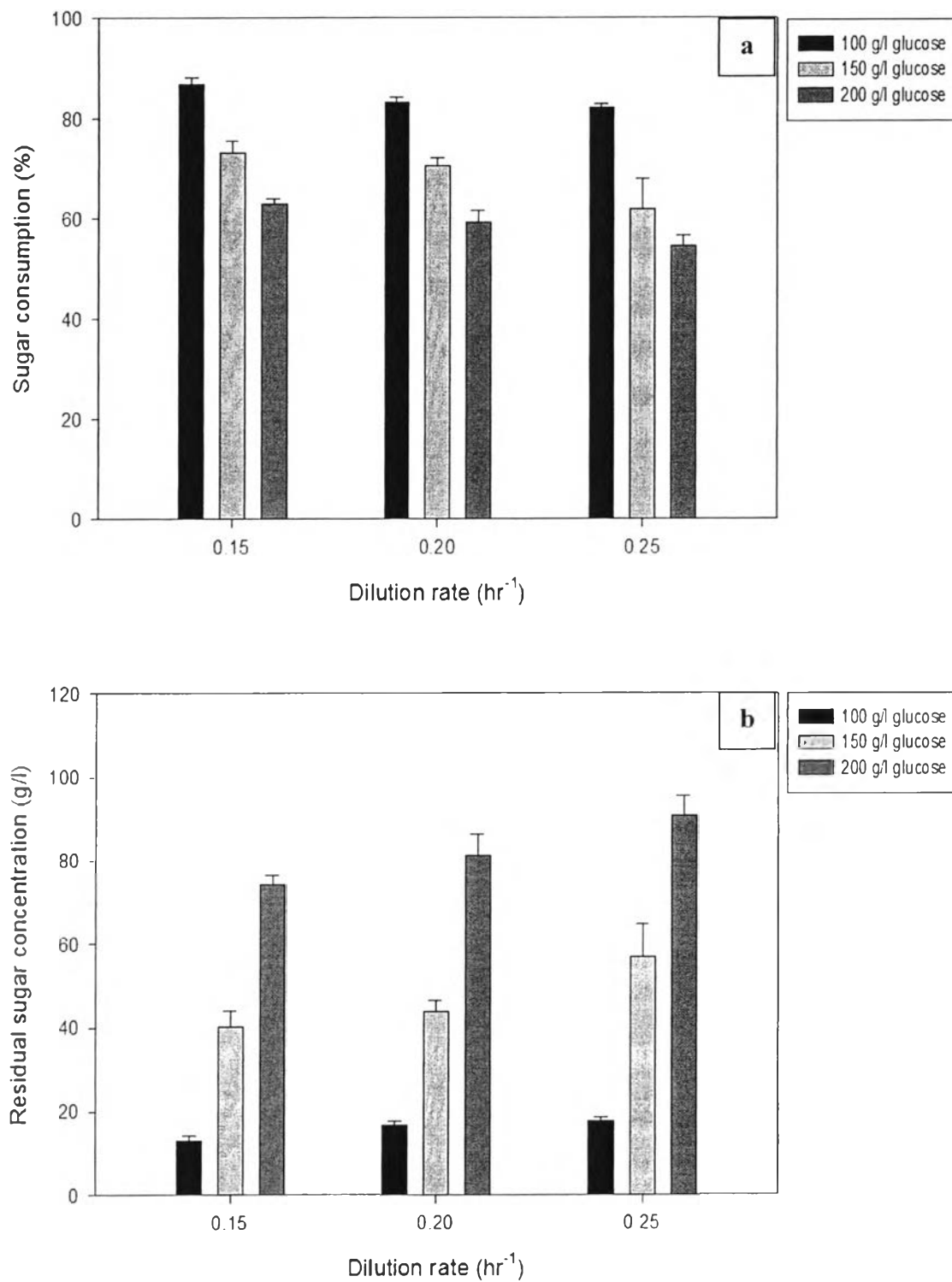


Figure 4.21 The effect of feed glucose concentration and dilution rate on (a) % sugar consumption and (b) residual sugar concentration.

4.4.4.3 A Comparison of the Fermentation Condition and Ethanol Production

Table 4.7 showed a comparison of the fermentation condition and ethanol production. In this work, the maximum ethanol yield equals to 0.48 at $6.20 \text{ gl}^{-1} \text{ hr}^{-1}$ of volumetric ethanol productivity (Q_p). This value was satisfied when it was compared with many previous works.

Table 4.7 A comparison of the fermentation condition and ethanol production

Author	Fermentation process	Yeast cell condition	Carrier		Max $Y_{P/S}$ (g/g)	Q_p ($\text{gl}^{-1} \text{hr}^{-1}$)
			Material	Method		
Kiran <i>et al.</i> , 2000	Batch	Immobilized cell	Ca-alginate	Entrapment	0.46	1.94
Nigam <i>et al.</i> , 2000	Continuous	Free cell	-	-	0.42	3.80
Laopaiboon <i>et al.</i> , 2009	Batch	Free cell	-	-	0.45	1.52
Ariyajaroenwong <i>et al.</i> , 2011	Continuous	Immobilized cell	Sweet sorghum stalk	Adsorption	0.47	1.30
Ghorbani <i>et al.</i> , 2011	Continuous	Immobilized cell	Ca-alginate	Entrapment	0.24	2.39
Razmovski <i>et al.</i> , 2012	Batch	Immobilized cell	Maize stem ground tissue	Adsorption	0.49	0.74
Vesna <i>et al.</i> , 2012	Batch	Immobilized cell	Sugar beet pulp	Adsorption	0.46	0.92
This work 2013	Continuous	Immobilized cell	SF/CLWs bionanocomposite sponge	Entrapment	0.48	6.20

4.5 Conclusions

The SF/CLWs bionanocomposite sponges were fabricated by freeze-drying silk fibroin solution containing cellulose whiskers at different SF/CLWs weight ratios in order to obtain a porous material with interconnected pores. The incorporation with high CLWs content into SF sponge causing intermolecular hydrogen bond between $-OH$ of CLWs and $-NH_2$ and/or $-OH$ of SF and inducing beta-sheet conformation of SF resulted in good water stability of SF/CLWs bionanocomposite sponge. Furthermore, the increase in the CLWs content caused higher water stability, less shrinkage, and better mechanical properties of SF/CLWs bionanocomposite sponges. The methanol-treated bionanocomposite sponges had better water stability than non-treated ones because methanol treatment can significantly enhanced the conformation transition from random coil to beta-sheet structure of SF sponge. The SF/CLWs bionanocomposite sponge fabricated at the SF/CLWs ratio of 50:50 (MSF50) provided the largest average pore size about $112.65 \mu\text{m}$ and contained the highest number of yeast cells around 3.80×10^{10} cells/1g of sponge. The MSF50 bionanocomposite sponge was chosen as a carrier for yeast cell immobilization using in continuous ethanol fermentation because MSF50 had highest pore size, water stability, dimensional stability, yeast cell density and lowest cell leakage. The continuous fermentation system was operated by the following operating condition: temperature at $30 \text{ }^\circ\text{C}$, pH at 4.5-5, feed sugar concentrations of 100, 150, and 200 g/l, dilution rate (D) of 0.15, 0.20 and 0.25 hr^{-1} . The ethanol production and volumetric ethanol productivity which obtained from fermentation increased when the feed glucose concentration increased but the % sugar consumption decreased. On the other hand, the ethanol production was decreased at high dilution rate because of less interaction time of glucose molecule with the immobilized yeast cells or low hydraulic retention time (H). The maximum ethanol production of 51.18 g/l with the volumetric ethanol productivity of $7.68 \text{ g l}^{-1} \text{ hr}^{-1}$ was obtained at 0.15 hr^{-1} dilution rate and 200 g/l feed glucose concentration. Finally, after finished fermentation SF/CLWs bionanocomposite sponge containing yeast cell can be as feed for animal because SF and yeast cell are excellent protein sources.

4.6 Acknowledgements

The authors would like to express their sincere gratitude to the Petroleum and Petrochemical College, Chulalongkorn University and the Center of Excellence on Petrochemical and Materials Technology for supporting this study.

4.7 References

- Alamri, H., and Low, I.M. (2012) Mechanical properties and water absorption behavior of recycled cellulose fibre reinforced epoxy composites. Polymer Testing, 31, 620–628.
- Rattanapan, A., Limtong, S., Phisalaphong, M. (2011) Ethanol production by repeated batch and continuous fermentations of blackstrap molasses using immobilized yeast cells on thin-shell silk cocoons. Applied Energy, 88, 4400–4404.
- Bai, F.W., Anderson, W.A., and Moo-Young, M. (2008) Ethanol fermentation technologies from sugar and starch feedstocks. Biotechnology Advances, 26, 89–105.
- Baimark, Y., Srisa-ard, M., and Srihanam, P. (2010) Morphology and thermal stability of silk fibroin/starch blended microparticles. EXPRESS Polymer Letters, 4(12), 781–789.
- Bangrak P. (2007) Continuous ethanol production using immobilized yeast cells entrapped in loofa reinforced alginate carriers. Faculty of Engineering Chulalongkorn University.
- Bayrock, D.P. and Ingledew, W. M. (2001) Application of multistage continuous fermentation for production of fuel alcohol by very-high-gravity fermentation technology. Journal of Industrial Microbiology & Biotechnology, 27, 87–93.
- Cao, Y. and Wang, B. (2009) Biodegradation of Silk Biomaterials. International Journal of Molecular Sciences, 10, 1514-1524.
- Daniel, P., Eliângela, M.T., Antônio, S.C., Mohamed, N.B., and Alain, D. (2010) Extraction of cellulose whiskers from cassava bagasse and their applications

- as reinforcing agent in natural rubber. Industrial Crops and Products, 32, 486–490.
- Eliangela, M.T., Thalita, J.B., Kelcilene, B.R.T., Ana, C., and Luiz, H.C.M. (2011) Sugarcane bagasse whiskers: Extraction and characterizations. Industrial Crops and Products, 33, 63–66.
- Fujii, N., Sakurai, A., Onjoh, K., and Sakakibara, M. (1999) Influence of surface characteristics of cellulose carriers on ethanol production by immobilized yeast cells. Process Biochemistry, 34, 147–152.
- Galbe, M., and Zacchi, G. (2002) A review of the production of ethanol from softwood. Appl Microbiol Biotechnol, 59, 618–628.
- Ghorbani, F., Younesi, H., Sari, A.E., and Najafpour, G. (2011) Cane molasses fermentation for continuous ethanol production in an immobilized cells reactor by *Saccharomyces cerevisiae*. Renewable Energy, 36, 503-509.
- Gordon, F., John. M., and Ralph, R. (2002) Molecular Biology and Biotechnology. The Royal Society of chemistry.
- Inouye, K., Kurokawa, M., Nishikawa, S., and Tsukada, M. (1998) Use of Bombyx morisilk fibroin as a substratum for cultivation of animal cells. Journal of Biochemical and Biophysical Methods, 37, 159–164.
- Johansen, A., and James, M. (1986) Immobilization of yeast cells by internal gelation of alginate. Enzyme Microbial Technology, 8, 145-148.
- Julien, B., Mohammad, L.H., Cecile, B., Enas, A.H., Nahla, A., and Alain, D. (2010) Mechanical, barrier, and biodegradability properties of bagasse cellulose whiskers reinforced natural rubber nanocomposites. Industrial Crops and Products, 32, 627–633.
- Kevin, A., Lishan, Z., and Mark, E. (2006) Bioethanol. Chemical Biology, 10, 141–146.
- Madigan, M.T., Martinko, J.M., and Parker, J. (2000) Nutrition and metabolism. Brock Biology of Microbiology.
- Michael, I. (2008) Cellulose as a nanostructured polymer: A short review. Bioresource, 1403-1418.
- Minoura, N., Aiba, S. I., Higuchi, M., Gotoh, Y., Tsukada, M., and Imai, Y. (1995) Attachment and growth of fibroblast cells on silk fibroin. 208(2), 511-516.

- Mondal, M., Trivedy, K., and Kumar, S. N. (2007) The silk proteins, sericin and fibroin in silkworm, *Bombyxmori* Linn., - a review. Caspian Journal of Environmental Science, 5(2), 63-76.
- Nurain, J., Ishak, A., and Alain, D. (2012) Extraction, preparation and characterization of cellulose fibres and nanocrystals from rice husk. Industrial Crops and Products, 37, 93–99.
- Razmovski, R., and Vucurovic, V. (2011) Ethanol production from sugar beet molasses by *S. cerevisiae* entrapped in an alginate-maize stem ground tissue matrix. Enzyme and Microbial Technology.
- Rosaa, M.F., Medeiros, E.S., Malmonge, J.A., Gregorski, K.S., Wood, D.F., Mattoso, L.H.C., Glenn, G., Ortsb, W.J., and Imam, S.H. (2010) Cellulose nanowhiskers from coconut husk fibers: Effect of preparation conditions on their thermal and morphological behavior. Carbohydrate Polymers, 81, 83–92.
- Salmon, J.M. (1996) Sluggish and stuck fermentations: some actual trends on their physiological basis. Vitic. Enol. Sciences, 51, 137-140.
- Samir, A., Alloin, F., and Dufresne, A. (2005) Review of recent research into cellulosic whiskers, their properties and their application in nanocomposite field. Biomacromolecules, 6, 612-626.
- She, Z., Jin, C., Huang, Z., Zhang, B., Feng, Q., and Xu, Y. (2008) Silk fibroin/chitosan scaffold: preparation, characterization, and culture with HepG2 cell. J Mater Sci: Mater Med, 19, 3545–3553.
- Shelley, D., and Minter. (2006) Alcoholic Fuels: An overview. Alcoholic Fuels, 1-4.
- Srisuwanand, Y. and Baimark, Y. (2011) Silk fibroin/chitosan blend films preparation and cross-linking by polyethylene diglycidyl ether. International Journal of Applied Chemistry, 7(3), 273-283.
- Um, I.C., Kweon, H.Y., Park, Y.H., and Hudson, S. (2001) Structural characteristics and properties of the regenerated silk fibroin prepared from formic acid. International Journal of Biological Macromolecules, 29, 91–97.
- Unger, R. E., Wolf, M., Peters, K., Motta, A., Migliaresi, C., Kirkpatrick, C. J. (2004) Growth of human cells on a non-woven silk fibroin net: a potential for use in tissue engineering. Biomaterials, 25, 1069–1075.

- Vepari, C. and Kaplan, D. L. (2007) Silk as a Biomaterial. Program Polymer Science, 32(8-9), 991–1007.
- Vesna, M., and Radojka, N. (2012) Sugar beet pulp as support for *Saccharomyces cerevisiae* immobilization in bioethanol production. Industrial Crops and Products, 39, 128–134.
- Wongpanit, P., Sanchavanakit, N., Pavasant, P., Bunaprasert, T., Tabata, Y., and Rujiravanit, R. (2007) Preparation and characterization of chitin whisker-reinforced silk fibroin nanocomposite sponges. European Polymer Journal, 43, 4123–4135.
- Wu, J. H., Wang, Z., and Xu, S. Y. (2007) Preparation and characterization of sericin powder extracted from silk industry waste water. Food Chemistry, 103, 1255–1262.
- Zaldivar, J., Nielsen, J., and Olsson, L. (2001) Fuel ethanol production from lignocellulose: a challenge for metabolic engineering and process integration. ApplMicrobiolBiotechnol, 56, 17–34.
- Zuluaga, R., Putaux, J.L., Cruz, J., Velez, J., Mondrago, I., and Ganán, P. (2009) Cellulose microfibrils from banana rachis: Effect of alkaline treatments on structural and morphological features. Carbohydrate Polymers, 76, 51-59.
- Zuluaga, R., Putaux, J.L., Restrepo, A., Mondragon, I., and Gañán, P. (2007) Cellulose microfibrils from banana farming residues: isolation and characterization. Cellulose, 14(6), 585-592.